IV. Transport Phenomena

The previous sections have illustrated how orderly and chaotic processes are inherent modes of many systems. Relatively simple systems with few degrees of freedom attain the different regimes according to the strength of some characteristic system parameter. Very complex systems, for example, multi-particle systems have a natural tendency to chaoticity. It was shown, how successive scattering processes mediated by interactions between particles in a dilute system (a gas) have a high sensitivity to initial conditions and produce random motion of the particles after only a few collisions. Once a system has entered the chaotic regime, it becomes in principle impossible to follow the equations of motion of all particles, even for a moderately small system size. Complex systems with particles prohibit in general a microscopic treatment of the dynamics of all particles already for technical reasons. Here, one can at most sample the behavior of the system by considering a representative subset of the total particle ensemble.

Fortunately, often the behavior of the individual particles is not of practical interest, and it is mostly the average, effective behavior of all particles together what actually counts. It is of interest, how the averages of certain observables behave, and perhaps the degree to which the actual variables fluctuate about the average trajectory.

The definitions of average and fluctuations refer to the moments of a probability distribution of the corresponding variables. For example, the macroscopic pressure of a gas sample, or the concentration of a reagent in a solution may change in time. This average behavior can be orderly, ***synergistic and self-organizing***, as exemplified by the oscillatory behavior of certain auto-catalytic chemical reactions (cf. Sect. II.1.2), and it can be completely or partially ***random***. The transition between the two domains is the result of dynamical transport processes such as ***diffusion, convection,*** and ***dissipation***. This transition is in essence unidirectional, from the more orderly to the more chaotic. The time evolution of these transport processes, resulting in a ***time-dependent probability distribution*** f of the variables describing the system, will be considered next.

IV.1. Master, Fokker-Planck and Diffusion Equations

In the following, the system of interest will be described in terms of the multi-variate probability distribution $\boldsymbol{f(q_i;t)}$ of all variables q_i describing the macroscopic, average state of the system as a function of time t. In general, probability can never be created or lost, it flows from one domain to the other, in certain ways like an incompressible liquid. As an example, one may consider a multi-particle system, where the probability (density) is defined as the number dN of particles per volume element dV

$$f(\vec{r}) = \frac{dN}{dV} \tag{IV.1}$$

and a probability current as the flow of particles with velocity $\vec{u}$

$$\vec{j} = \frac{dN}{dV} \cdot \frac{d\vec{r}}{dt} = f \cdot \vec{u} \tag{IV.2}$$

In terms of probability and associated current, one can formulate a

Continuity Equation

$$\frac{df}{dt} = \frac{\partial f}{\partial t} + \vec{\nabla} \cdot \vec{j} = 0 \tag{IV.3}$$

well known also from quantum mechanics. This equation states the ***conservation of probability*** mathematically in terms of the total time derivative, which vanishes, i.e., $df/dt = 0$. The total derivative is the sum of the partial derivative of f with respect to time, $\partial f / \partial t$,

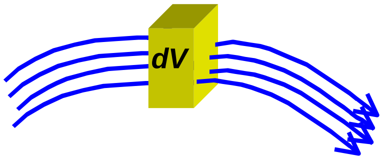

Figure IV-1: Probability flow.

testing for an explicit time dependence of *f*, and the divergence term describing the change of probability at the given position, just due to the probability flow through the volume element of interest. The continuity equation states, hence, that the time dependence of the probability is due to the fact that the gradient of the probability current $\vec{j}$ is non-zero. For example, the time dependence is a ***gain*** in probability, if the current gradient is negative, $\vec{\nabla}\cdot\vec{j}<0$. For $\vec{\nabla}\cdot\vec{j}=0$, as shown in Fig. IV.1, there is no change in the probability to find a particle in the volume element pictured.

To discuss a simple example more specifically, let the probability flux be one-dimensional, such as indicated in Fig. IV.2. This is both an application of the Continuity Equation and an illustration of its self-evidence.

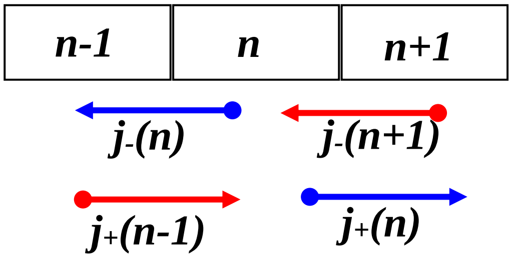

Figure IV-2: Probability balance, one dimension.

The probability currents in positive and negative direction are denoted by j_+ and j_-, respectively. Divide further the one-dimensional space into discrete bins numbered *n*. Consider now the time-dependent probability $f_n(t)$ for bin *n* (probability to find a particle in this bin *n* at time *t*). This bin receives and transmits probability from and into the neighboring bins, *n+1* and *n-1*, respectively. Origin and direction of these flows or currents are indicated by the arrows in the figure. There are obviously only four different currents involving bin *n*, to and from the bin and in either direction.

The balance of probability in bin *n* can be calculated as

$$\frac{\partial f_n(t)}{\partial t} = -\left| j_+(n,t) - j_+(n-1,t) \;+\; j_-(n+1,t) - j_-(n,t) \right| \qquad \text{(IV.4)}$$

This is intuitively clear and follows also from the Continuity Equation IV.3. The differences are just representations of the corresponding current gradients

$$\vec{\nabla}\cdot\vec{j} = \vec{\nabla}\cdot\left(\vec{j}_- - \vec{j}_+\right) = \Delta j_+ - \Delta j_- . \qquad \text{(IV.5)}$$

to be inserted into Equ. IV.3. The first bracket term in Equ. IV.4 describes the ***net loss of probability*** from bin *n*, the second the ***net gain in probability*** by this bin. Using the product form of the currents given by Equ. IV.2, one can rewrite Equ. IV.4 as

$$\frac{\partial f_n(t)}{\partial t} = \; u_+(n-1) f_{n-1}(t) + u_-(n+1,t) f_{n+1}(t) \;-\; u_+(n) + u_-(n,t) \;\; f_n(t) \qquad \text{(IV.6)}$$

The velocities u_+ and u_- play the role of ***transition probabilities*** for particles between different bins, e.g.,

$$w_{n\rightarrow n+1} \propto \frac{1}{\Delta t} \propto \frac{u_+}{\Delta n} = u_+ \qquad \text{(IV.7)}$$

It is reasonable to assume that these transition probabilities are characteristic only for the different bins which they connect but do not dependent on time nor on the probabilities f_n to find particles in each bin. Then, one can rewrite Equ. IV.6 as a

The above equation has been derived for the case, where bin *n* is connected only to the nearest neighbors, with every summation index having only the two values $m = n \pm 1$. However, one can trivially include the case of *m* = *n*, which contributes zero to the sum. One can also extend the summation *m* to all possible states, if transition probabilities can connect these states. Furthermore, it is not necessary to consider the Master Equation as a one-dimensional transport equation. Each state can be characterized by an entire set of variables, such that the bin ***number n represents an entire set of coordinates***. For example, it is trivial to show the validity of the two-dimensional Master Equation for transitions on a two-dimensional *x*-*y* grid, where the two coordinates are represented by separate bin numbers:

Master Equation

$$\frac{\partial}{\partial t} f_n(t) = \sum_m \left\{ w_{m\to n} f_m(t) - w_{n\to m} f_n(t) \right\} \qquad \text{(IV.8)}$$

$$\frac{\partial}{\partial t} f_{n,n'}(t) = \sum_{m,m'} \left\{ w_{m,m'\to n,n'} f_{m,m'}(t) - w_{n,n'\to m,m'} f_{n,n'}(t) \right\} \qquad \text{(IV.9)}$$

The Master Equation is a general ***classical rate equation*** describing the change in the population of a state (here of bin *n*) via transitions to and from this state, from and to other states of the system. It is classical in the sense that it neglects interference terms in the quantal transition amplitudes and presumes an absence of particle correlations, e.g., the ***Pauli Principle*** which would block transitions to an extent that the final states are already occupied with some probability. In an approximate manner, the effects of this "***Pauli***

blocking" can be taken into account by multiplying the transition probabilities $w_{n\to m}$ in Equ. IV.8 by the blocking factors $(1-f_m)$ representing the probabilities that a final state *m* is available for the transition $n \to m$.

The Master Equations IV.8 or 9 represent prescriptions of how to propagate from an initial set of probabilities $\{f_n(t=0)\}$ at *t=0* to a final distribution of probabilities $\{f_n(t\neq 0)\}$ over the accessible states. Since it allows the system to make transitions from a single given initial state to several, perhaps many, other states, the effect is a spreading in time of the probability over many states. Hence, the Master Equation describes a ***dissipative process***. A two-dimensional dissipation process is illustrated schematically by Fig. IV.3 below and an animation, both produced with the code MATHCAD_252\Random_Walk.mcd. The calculation assumes that at *t=0*, all probability is in a single state, the center bin of a two-dimensional x-y grid. From here, transitions are possible to states chosen at random with probabilities that are equal within a given distance of a bin from the center. As can be seen, the probability spreads out from the initial center-bin population to fill most of the

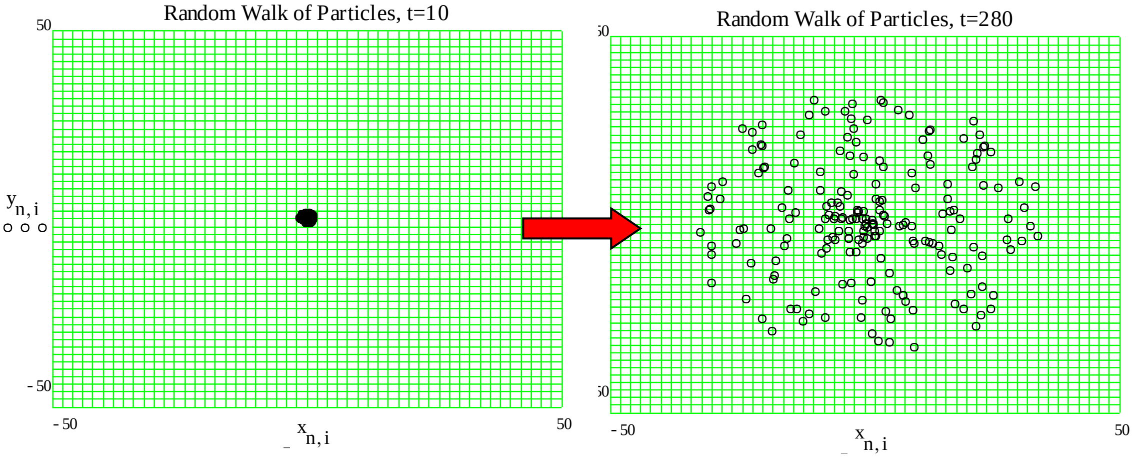

Figure IV-3: Two-dimen. random walk of 200 particles

available space. The animation illustrates the changing speed of dissipation. The probability spreads very fast at first, but at later stages of the process, it takes more time to fill the space evenly. This is to be expected, as the accessible space becomes larger and larger in each step.

The tendency of spreading probability in a dissipative process can be visualized most readily in a one-dimensional case, the simplest interpretation of Equ. IV.8. A further assumption that the probability, $w_{n,m} := w_{n\to m} = w_{m\to n} =: w_{m,n}$, for populating and depopulating, is often fulfilled, if not demanded by quantum-mechanical rules. The Master Equation for such a simple case reads

$$\frac{\partial}{\partial t} f_n(t) = \sum_m w_{m,n}\left\{ f_m(t) - f_n(t)\right\} = \begin{cases} >0 & f_m > f_n \\ <0 & f_m < f_n \end{cases} \qquad \text{(IV.10)}$$

This implies that bins *n* receive probability from all other cells *m*, whose population is larger than that of bin *n*. Bin *n* transfer probability to all other bins *m* that have a smaller population than bin *n*. Eventually, when all bins have the same average probability, $f_m \approx f_n$, the dissipation process described by the Master Equation comes to a halt. This implies that ***asymptotically, for*** $t \to \infty$***, the system attains equilibrium with an equipartition of the probability*** among all accessible states:

$$\lim_{t\to\infty} f_n(t) = \left(f_n\right)_{equ} = const. \qquad \text{(IV.11)}$$

Transport processes are often called ***equilibration and relaxation*** processes, since they lead a system that is initially very far from equilibrium to its final equilibrium state, given enough time.

Equation IV.11 represents an operational definition of the situation of thermal equilibrium: On average, the probabilities for different micro-states are all equal and do not change in time. However, in each for each sampling measurement, the actual populations of the states may vary from the average. That the Maxwell-Boltzmann distribution of the positions of gas particles at equilibrium have equal probabilities, whereas the corresponding velocities appear with very different probabilities, is not a contradiction to this principle. States (or bins) with different velocities are not equivalent. In a collision process, high velocities are not produced as readily as low and intermediate velocities.

The explicit form of the Master Equation IV.8 containing the probabilities of all states, as well as all connecting transition probabilities for all times, makes it a very flexible equation of motion for a large class of systems. It also lends itself easily to realistic simulations of the transport processes. However, it is also very difficult, if not impossible, to solve accurately for system with many degrees of freedom. Therefore, approximation methods have been developed that allow analytical solutions for quasi-continuous processes. Such methods transform the Master Equation to a Fokker-Planck or a so-called diffusion equation.

In the following, for simplicity the one-dimensional process described in Equ. IV.6 is considered again. However, it is now assumed that the velocities u_+ and u_- and the probabilities f_n are ***continuous functions*** of the bin number n. This is a particularly good assumption for spatial degrees of freedom, which are naturally continuous. The assumption is also valid for energies that are high enough, such that the quantal energy spectrum which is discrete at low energies has degenerated into a classical continuum.

Under these conditions, one can expand terms in Equ. IV.6 in a Taylor expansion up to second order to obtain the corresponding Fokker-Planck Equation. Specifically, one replaces the probability currents j_+ and j_- by such Taylor expansions:

$$u_+(n-1)\,f_{n-1}(t)-u_+(n)\,f_n(t)\;\approx -\frac{\partial}{\partial n}\left[u_+(n)\,f_n\right]+\frac{1}{2}\frac{\partial^2}{\partial n^2}\left[u_+(n)\,f_n\right]$$

and

(IV.12a)

$$u_-(n+1)\,f_{n+1}(t)-u_-(n)\,f_n(t)\;\approx \frac{\partial}{\partial n}\left[u_-(n)\,f_n\right]+\frac{1}{2}\frac{\partial^2}{\partial n^2}\left[u_-(n)\,f_n\right]$$

(IV.12b)

Adding the two above equations IV.12a and b, one regains, from the terms on the *l.h.s.* of Equs. IV.12, Equ. IV.6 for the partial time derivative of the probability f_n and a second-order approximation to it, from the terms on the *r.h.s.* The resulting equation for the time-dependence of the probability has the form of a

Fokker-Planck Equa-

$$\boxed{\frac{\partial}{\partial t}f_n(t)=-\frac{\partial}{\partial n}\left[v_n f_n(t)\right]+\frac{\partial^2}{\partial n^2}\left[D_{nn} f_n(t)\right]} \qquad \text{(IV.13a)}$$

Here, ***the transport coefficients contain the scientific information on the transport process***. They are defined as

$$\begin{aligned} v_n &= u_+(n) - u_-(n) \quad \textit{Drift Coefficient} \\ D_{nn} &= \frac{1}{2}\left(u_+(n) + u_-(n)\right) \quad \textit{Diffusion Coefficient} \end{aligned} \qquad \text{(IV.13b)}$$

The drift coefficient describes the difference in the probability currents j_+ and j_-, while the diffusion coefficient represents an average undirected ***mobility*** of the system.

For constant transport coefficients, which do not depend on the bin position n, $v_n = const.$ and $D_{nn} = const.$, the Fokker-Planck Equation has Gaussian solutions:

$$f_n(t) = \frac{1}{\sqrt{2\pi\sigma_n^2(t)}} \exp\left\{-\frac{\left(n - \bar{n}(t)\right)^2}{2\sigma_n^2(t)}\right\} \qquad \text{(IV.14)}$$

This can be proven by inserting the normalized function IV.14 into the Fokker-Planck Equation. Here, $\bar{n}(t)$ is the average n (the first moment) and $\sigma_n^2(t)$ is the variance in n (the second moment). Both moments are defined with respect to the probability distribution of Equ. IV.14, both are time dependent quantities. The average indicates the position of the Gaussian probability distribution, while the variance indicates its width. Both $\bar{n}(t)$ and $\sigma_n^2(t)$ are linear functions of time:

$$\begin{aligned} \bar{n}(t) &= \bar{n}(0) + v_n \cdot t \\ \sigma_n^2(t) &= \sigma_n^2(0) + 2D_{nn} \cdot t \end{aligned} \qquad \text{(IV.15)}$$

The Gaussian probability distribution of Equ. IV. drifts to the side with constant velocity, while it broadens. It is interesting to note that the ***drift and width grow in a correlated fashion***, independent of time. Specifically, the ratio of first and second moment of the probability distribution for the variable *n* is a constant:

$$\frac{\Delta\bar{n}(t)}{\sigma_n^2(t)} = \frac{\bar{n}(t)-\bar{n}(0)}{\sigma_n^2(t)-\sigma_n^2(0)} = \frac{v_n}{2D_{nn}} = const. \qquad \text{(IV.16)}$$

Figure IV.4 shows as an example of a Fokker-Planck process the

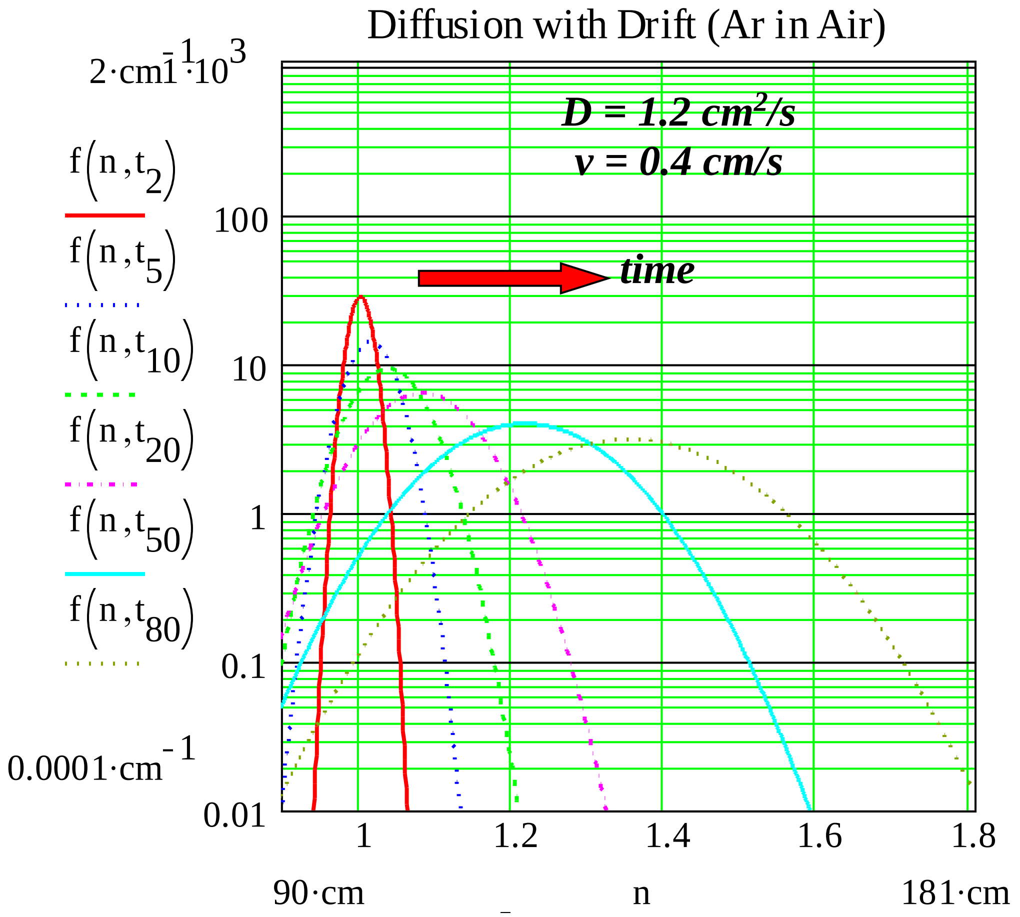

Figure IV-4: Fokker-Planck diffusion and drift of Ar ions in air with applied electrostatic potential

diffusion of argon ions in air at *25°C*, as given by Equ.IV.14, with a realistic diffusion coefficient of *D=1.2 cm²/s* and a large drift coefficient of $v=0.4cm/s$, the latter due, e.g., to some applied external electric field. (MATHCAD_252\Fokker_Planck_Sol.mcd) Shown is a time span of only *80 s* after the release of the *Ar* into the atmosphere. With increasing time, the *Ar* ions are seen to disperse in space and, as a whole, drift to the right. After only a minute or so, the half width of the probability distribution has increased to the order of *0.5 m*. The process can be also be viewed dynamically. The animation suggests ways to determine experimentally the two transport coefficients by measuring two moments of the probability distribution developing as a function of time.

Of course, if the space of the variable *n* is homogeneous, the probability currents $\dot{j}_+$ and $\dot{j}_-$ are equal, and the drift coefficient vanishes, $v_n=0$. Then, there is no reason for the probability distribution to drift in time to one side, although it will still become broad in time. For vanishing drift coefficient, the Fokker-Planck Equation IV.13 degenerates to the

Diffusion Equation

$$\frac{\partial}{\partial t} f_n(t) = D_{nn} \frac{\partial^2}{\partial n^2} f_n(t) \qquad \text{(IV.17)}$$

This diffusion equation has a simple structure. The time-rate of change of the probability f_n is proportional to the diffusion coefficient D_{nn}. The larger in magnitude the diffusion coefficient, the faster the probability f_n will change in time. The ***rate of change of*** f_n ***is also proportional to the spatial curvature of*** f_n, *not* its gradient. As an immediate consequence of this feature, one concludes that, if the probability f_n has a linear dependence on *n* anywhere, the probability remains linear. For example, a constant probability $f_n = const.$

will not be influenced by the diffusion process. Each bin receives as much probability from its neighbors as it transmits to them. This behavior is consistent with the fact that the drift coefficient is zero and the eventual attainment of equilibrium.

Of course, a non-zero slope of the probability would induce a flow from the higher to the lower probability and hence an average drift. According to ***Fick's (empirical) Law*** a gradient in concentration (probability) *f* always leads to an average current *j* flowing in the direction of the steepest gradient and whose effect is to eventually eliminate that gradient:

$$\vec{j} = -D\vec{\nabla} f \qquad \text{(IV.18)}$$

where *D* is the diffusion coefficient indicating the mobility of the carriers of the property of interest. It is easy to see that Fick's Law is consistent with the diffusion equation, because from Equ. IV.18, it follows that

$$\vec{\nabla}\cdot\vec{j} = -D\vec{\nabla}\cdot\vec{\nabla} f = -D\Delta f \qquad \text{(IV.19)}$$

Here, *Δ* is the Laplacian differential operator, defined in Cartesian spatial dimensions {*x*,*y*,*z*} as $\Delta = \vec{\nabla}\cdot\vec{\nabla} = \left\{\frac{\partial^2}{\partial x^2} + \frac{\partial^2}{\partial y^2} + \frac{\partial^2}{\partial z^2}\right\}$

Using the continuity equation, one derives from Equ. IV. 20 with just one dimension *n:*

$$\frac{\partial}{\partial t} f_n(t) = -\vec{\nabla}\cdot\vec{j} = +D\frac{\partial^2}{\partial n^2} f_n(t) \qquad \text{(IV.20)}$$

Equ. IV.20, however, is exactly the diffusion equation derived earlier. Taking the gradient of Fick's equation leads to the diffusion equation. What gets lost in the comparison are components of the probability current which are constant with respect to the spatial variables and have zero derivatives. Such currents are, however, included in the Fokker-Planck Equation with non-zero drift coefficients. Hence, the latter equation is the more appropriate equation of motion to use for the probability, if there is an initial linear variation of *f* about its average.

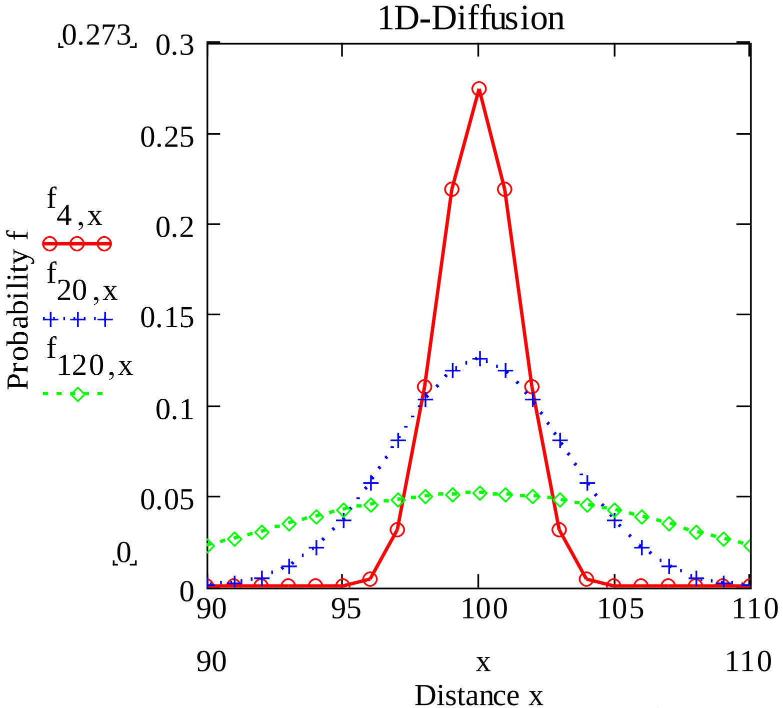

Figure IV-5: Time evolution of probability

The diffusion equation has Gaussian solutions, like the Fokker-Planck equation, except that, for the simpler diffusion case, there is no average drift of the entire probability distribution in time. Consequently, the probability distribution does not drift away in time from its initial position, but simply broadens. The solutions to the diffusion equation are Gaussians of the form of Equ. IV.14, however, with a fixed average value $\bar{n}(t) = \bar{n}(0)$, as seen in the example of Fig. IV.5, calculated for a schematical case (MATHCAD_252\1D_Diffusion.mcd).

In the animation of this diffusion process, one observes again a very rapid change (broadening) of the concentration of the probability at first, when the probability has a large curvature (second spatial derivative), followed by a more gradual decay. In view of the above discussion of Fick's Law and the structure of the solutions (Equs.

IV.14 and IV.15), this is no surprise. The variance increases in proportion to the time elapsed in the diffusion process. Therefore, the width, which is proportional to the standard deviation (see Tutorial), the square-root of the variance, changes with the square-root of time.

In Fig. IV.5, one observes a Gaussian probability distribution for the position *x*,

$$f(x,t) = \frac{1}{\sqrt{2\pi\sigma_x^2(t)}} \exp\left\{-\frac{(x-\bar{x})^2}{2\sigma_x^2(t)}\right\} \qquad \text{(IV.21a)}$$

with average position $\bar{x} =: \langle x \rangle$ and a variance in position *x* given by

$$\sigma_x^2(t) = \left\langle x^2 \right\rangle - \left\langle x \right\rangle^2 = \sigma_x^2(0) + 2D_{xx}\cdot t \qquad \text{(IV.21b)}$$

It is no surprise that the only non-zero moments of the probability distribution defined by Equ. IV.21a are the first and second moments and that only the second moment is time dependent. The corresponding differential equation does not contain any information other than on the curvature of the spatial probability function.

Choosing the origin of the *x*-axis appropriately, such that the average position is at zero, i.e., $\langle x \rangle = 0$, and starting with a vanishing initial variance, $\sigma_x^2 = 0$, one has the experimentally interesting relation

$$D_{xx} = \frac{1}{2\cdot t}\sigma_x^2(t) = \frac{1}{2\cdot t}\left\langle x^2 \right\rangle = \frac{1}{2\cdot t}x_{rms}^2 \qquad \text{(IV.22)}$$

This equation implies that the average, *rms* displacement of the particles in a diffusing sample grows only with the square root of time,

$$x_{rms} = \sqrt{2 \cdot D_{xx} \cdot t} \qquad \text{(IV.23)}$$

Equation IV.23 allows one also to determine the diffusion coefficient from experimental values for the *rms* distance x_{rms} , the square-root of the variance $\sigma_x^2 = \langle x^2 \rangle$, at time *t* of the particles from their point of origin at *t=0*.

One can now obtain an estimate for diffusion coefficients in the gas phase from the earlier discussion of molecular collisions. Consider particles of type *A* diffusing in a gas of particles of type *B* at equilibrium temperature *T*. It is reasonable to assume that particles *A* attain equilibrium with the other gas particles *B* very quickly. Then, one can apply the results of Section III.4. The total mean-square displacement x_{rms}^2 of a particle *A* depends on the number of collisions $N_{AB}(t)$ with particles *B* and the mean-square displacement $x_{i,rms}^2 \approx \lambda^2$ associated with each of the N_{AB} collisions that have occurred up to time *t*. Since, in the present approximation, all of these collisions are thought to be independent of each other, the variances $\left(\sigma_x^2\right)_i = x_{i,rms}^2$ of the distribution of displacements after each collision simply add up (see also Tutorial Moments):

$$x_{rms}^2 = \sum_{i=1}^{N_{AB}(t)} x_{i,rms}^2 \approx N_{AB}(t) \cdot \lambda^2 \qquad \text{(IV.24)}$$

Here, λ is the mean free path for collisions *AB*, equal to the *rms* displacement. Adapting the collision rate calculated in Equ. III.89 for one particle *A*, one has

$$N_{AB}(t) = \rho_B \langle u_{AB} \rangle \cdot \sigma_{AB} \cdot t \qquad \text{(IV.25)}$$

which can be inserted into Equ. IV.24, yielding

$$x_{rms}^2 \approx N_{AB}(t)\cdot\lambda^2 = \rho_B\langle u_{AB}\rangle\cdot\sigma_{AB}\cdot t\cdot\lambda^2 = \frac{\langle u_{AB}\rangle}{\rho_B\sigma_{AB}}\cdot t \qquad \text{(IV.26)}$$

Here, the notations are as usual for the particle number density ρ_B, the mean relative velocity $\langle u_{AB}\rangle$, and the collision cross section σ_{AB}. The characteristic relative (*rms*) velocity in *AB* collisions has already been deduced (cf. Equ. III.121)

$$D_{xx} = \frac{x_{rms}^2}{2t} \approx \frac{\langle u_{AB}\rangle}{2\rho_B\sigma_{AB}} = \frac{\sqrt{2k_BT}}{\sqrt{\pi\mu}\,\rho_B\sigma_{AB}} \qquad \text{(IV.27)}$$

where $\mu = \dfrac{m_A\cdot m_B}{m_A+m_B}$ is the reduced mass for the binary colliding system *AB*.

According to Equ. IV.27, the diffusion coefficient, representing some average mobility of particle *A* in gas *B*, increases with the root of the temperature. This is so, because the inherent velocity of particle *A* in thermal equilibrium increases with the root of *T*. Furthermore, the mobility is reduced for heavy particles, again because they are slower. The inverse dependence on density of the gas and the collision cross section also makes sense. The larger the product of these quantities, the more frequent are collisions within the gas, and the shorter are the distances that particle *A* travels, before its direction of flight is changed again.

For these reasons, diffusion coefficients are rather different for different materials. Some examples are listed in Table IV.1. Gases typically have diffusion coefficients of the order of $D \sim 10^0 cm^2/s$, with qualitatively the expected dependencies on size. Metals in molten, liquid form have coefficients that are many orders of magnitude smaller than that, $D \sim 10^{-14} cm^2 / s$. For the latter materials, measurements of transport coefficients use radioactive tracer methods.

Table IV-1: Experimental Diffusion Coefficients

System	D/cm^2s^{-1}	T/K	System	$D/10^{-5}cm^2s^{-1}$	T/K
He-He	2.38	275	Au in Ag	2.46	1253
$He-H_2$	0.25	90	In in Ag	3.81	1253
$He-N_2$	0.09	77	Sb in Ag	4.11	1253
$He-SF_6$	16.36	2900	Ag in Ag	$1.27\ 10^{-9}$	723
$Ne-H_2$	0.15	90	Co in Co	$0.95\ 10^{-9}$	1043
$Ne-N_2$	0.32	293	Fe in Fe	$21.1\ 10^{-9}$	1173

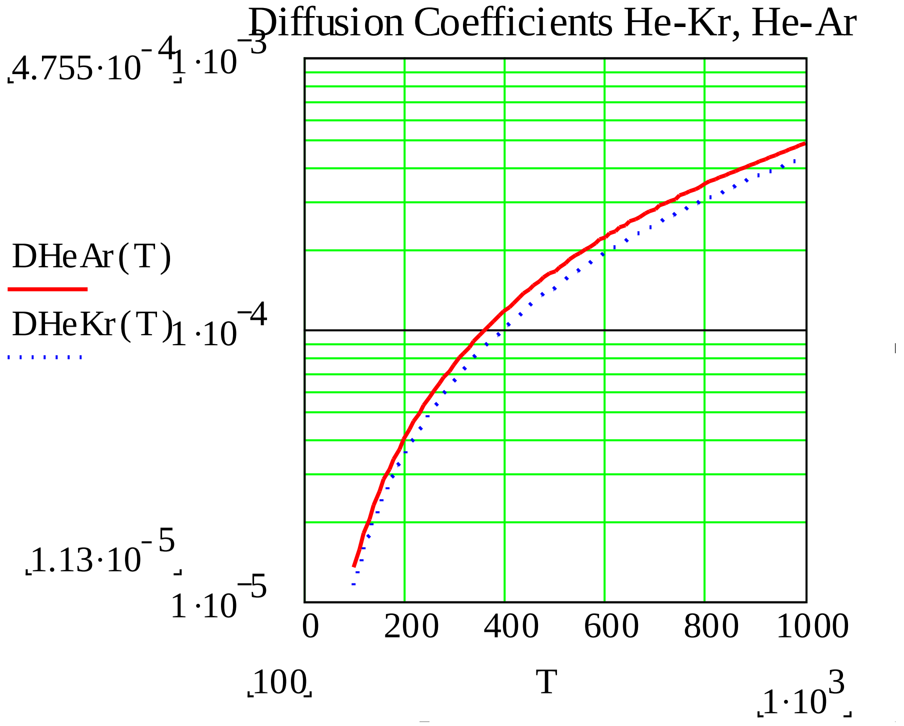

Figure IV-6: Temperature dependence of gas diffusion coefficients.

The **empirical** temperature dependence of two gas diffusion coefficients is plotted in Fig. IV.6. The dependence is qualitatively as expected. However, the experimental data increase faster than the square-root behavior expected.

For the purpose of numerical simulations used in this discussion to illustrate diffusive processes differential equations of motion can be converted into finite-difference equations. For example, the first time derivative of the probability density $f_n(t)$ is approximated by the difference equation

$$\left.\frac{\partial f_n(t)}{\partial t}\right|_{t=t_i} \approx \frac{f_n(t_i+\Delta t/2) - f_n(t_i-\Delta t/2)}{\Delta t} \approx \frac{f_n(t_{i+1}) - f_n(t_{i-1})}{2\Delta t} \tag{IV.28}$$

Analogously, the second spatial (*n*) derivative is approximated by the difference equation

$$\frac{\partial^2 f_n(t)}{\partial n^2} \approx \frac{\left[\frac{f_{n+1}(t) - f_n(t)}{2\Delta n}\right] - \left[\frac{f_n(t) - f_{n-1}(t)}{2\Delta n}\right]}{2\Delta n} = \frac{f_{n+1}(t) - 2f_n(t) + f_{n-1}(t)}{(2\Delta n)^2} \tag{IV.29}$$

In this approximation, the diffusion equation leads to the following iteration scheme for the probability

$$f_n(t_{i+1}) = f_n(t_i) + \frac{D_{nn}\Delta t}{(\Delta n)^2}\left[f_{n+1}(t) - 2f_n(t) + f_{n-1}(t)\right] \tag{IV.30}$$

Hence, the probability at spatial position n at time $t_{i+1} = t_i + \Delta t$ is determined by the spatial distribution of f at the earlier time t_i and the diffusion coefficient D_{nn}.